Phase sensitivity of a Mach-Zehnder interferometer with single-intensity and difference-intensity detection

Stefan Ataman[*]
Extreme Light Infrastructure-Nuclear Physics (ELI-NP), 'Horia Hulubei' National R&D Institute for Physics and Nuclear Engineering (IFIN-HH), 30 Reactorului Street, 077125 Măgurele, jud. Ilfov, Romania

Anca Preda[†]
Faculty of Physics, University of Bucharest, R-077125 Măgurele, Romania

Radu Ionicioiu[‡]
Horia Hulubei National Institute of Physics and Nuclear Engineering, 077125 Bucharest, Romania

(Received 25 June 2018; published 30 October 2018)

Interferometry is a widely used technique for precision measurements in both classical and quantum contexts. One way to increase the precision of phase measurements, for example, in a Mach-Zehnder interferometer (MZI), is to use high-intensity lasers. In this paper we study the phase sensitivity of a MZI in two detection setups (difference intensity detection and single-mode intensity detection) and for three input scenarios (coherent, double coherent, and coherent plus squeezed vacuum). For the coherent and double coherent input, both detection setups can reach the quantum Cramér-Rao bound, although at different values of the optimal phase shift. The double coherent input scenario has the unique advantage of changing the optimal phase shift by varying the input power ratio.

DOI: 10.1103/PhysRevA.98.043856

I. INTRODUCTION

Precision measurements are a key element in both science and technology. Indeed, many important discoveries have been made due to the improvement of measurement techniques. More sensitive instruments, like microscopes and telescopes, were paramount in discovering new phenomena and in verifying or falsifying theoretical predictions. Thus, improving the measurement sensitivity is a crucial factor driving the advancement of science and technology alike.

A very sensitive, hence widely used measurement technique is interferometry, with the Mach-Zehnder interferometer (MZI) as a standard tool. Thus, understanding, controlling and improving the limits of phase sensitivity of a MZI is an active field of research, both theoretically and experimentally [1–5].

Classically, the sensitivity $\Delta\varphi$ of a measurement is bounded by the standard quantum limit (SQL), also known as the shot-noise limit [4,6,7]. This is given by $\Delta\varphi_{\mathrm{SQL}} \sim 1/\sqrt{\langle N\rangle}$, where $\langle N\rangle$ is the average number of photons used to probe the system.

It was soon realized that squeezed states of light [8–10] can improve the phase sensitivity of an interferometer [11,12]. Indeed, this technique has been tested and is to be used at the LIGO detector in the future [3,13]. In a seminal article Caves [2] showed that squeezed light can improve the phase sensitivity of an interferometer below the shot-noise limit. Experimental demonstration with a MZI [14] soon followed, proving the usability of the concept in practical measurements. Over the following decades both theoretical and experimental studies showed how to improve the sensitivity of a MZI fed by both a coherent and a squeezed vacuum input [15–18].

In a quantum context, however, the phase sensitivity is bounded by the Heisenberg limit [4,11,19–21] $\Delta\varphi_{\mathrm{HL}} \sim 1/\langle N\rangle$ and this limit is fundamental [22]. The so-called NOON states [11,19,21] saturate this limit, while separable states obey the SQL [21].

The Heisenberg limit can be achieved in a MZI by injecting a coherent state in one port and squeezed vacuum into the other [23], if roughly half of the input power goes into squeezing. This result was confirmed by Lang and Caves [24,25], who, moreover, showed the input state to be optimal for the class of coherent plus squeezed vacuum type of states.

Other scenarios considering active SU(1,1)-type interferometers were studied in [26,27]. The authors showed a Heisenberg sensitivity limit achievable in a MZI with squeezed coherent light in both inputs, if the squeezing power is roughly 1/3 of the total power.

The phase sensitivity of a MZI is not constant [4]. For a small phase variation measurement, one can assume that the interferometer is preconfigured at a convenient point, where the sensitivity is maximal. In order to extend the (rather limited) range of values where each detection scheme approaches the Cramér-Rao bound, we can use a Bayesian approach and photon-number resolving detectors. The Cramér-Rao bound can be reached with this technique for any value of φ, as

[*]stefan.ataman@eli-np.ro
[†]anca.preda10@gmail.com
[‡]r.ionicioiu@theory.nipne.ro

shown by Pezzé *et al.* [28]. Moreover, this can be also achieved for the coherent plus squeezed vacuum input [23].

There are several detection methods used to measure the output of a MZI [29], however in this paper we focus only on two. In the difference intensity detection scheme, as the name suggests, we have two detectors (one for each output of the MZI) and we measure the difference of the two photocurrents. In the single-mode intensity detection scheme we measure only one photocount of the two. For low-power setups the difference intensity detection scheme is experimentally preferred. Here we show that for high input power, the single-mode detection scheme is superior to the difference intensity detection scheme.

We also consider the double coherent input case in this paper. This scenario was discussed by Shin *et al.* [30]. Moreover, we show that this scenario can have a practical interest under certain circumstances.

Although Heisenberg limited metrology has been a constant theoretical and experimental challenge, this favorable scenario happens for NOON states [11], where the current record in the number of photons remains very low [31,32] or at extremely low laser powers coupled with the highest squeezing factors achievable today. In this paper we are not interested in pursuing the Heisenberg limit at all costs. Instead we focus on scenarios where the squeezing factor is a limited resource, but the intensity of the coherent source is not constrained [3,33]. This setup is better suited to present-day experiments.

The paper is structured as follows. In Sec. II we introduce our parameter estimation method, experimental setup, field operator transformations, and output operator calculations. We also review the Cramér-Rao bound and the Fisher information approach. In Sec. III we consider a coherent plus vacuum input scenario and evaluate its phase sensitivity, comparing both output detection scenarios with the quantum Cramér-Rao bound. In Secs. IV and V we consider a coherent plus coherent input scenario and a coherent plus squeezed vacuum input scenario, respectively. We evaluate their respective phase sensitivities, compare the output detection scenarios, and assess them with respect to the quantum Cramér-Rao bound. All three scenarios are thoroughly discussed and conclusions are drawn in Sec. VI.

II. MZI SETUP: DETECTION SENSITIVITIES

A. Parameter estimation: A short introduction

We now briefly overview the problem of parameter estimation in quantum mechanics. An experimentally accessible Hermitian operator $\hat{O}$ depends on the parameter φ, which in our case is the phase shift in a Mach-Zehnder interferometer; by itself φ may or may not be an observable. The average of the operator is

$$\langle \hat{O}(\varphi)\rangle = \langle\psi|\hat{O}(\varphi)|\psi\rangle, \tag{1}$$

where $|\psi\rangle$ is the wave function of the system. A small variation $\delta\varphi$ of the parameter φ induces a change

$$\langle \hat{O}(\varphi+\delta\varphi)\rangle \approx \langle \hat{O}(\varphi)\rangle + \frac{\partial\langle \hat{O}(\varphi)\rangle}{\partial\varphi}\delta\varphi. \tag{2}$$

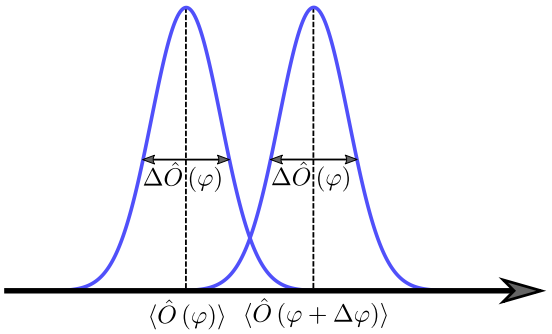

FIG. 1. Physical intuition behind Eq. (3). The sensitivity $\Delta\varphi$ depends on both the displacement of the average $\langle\hat{O}\rangle$ (due to a change of the parameter φ) and the standard deviation $\Delta\hat{O}$. Here we implicitly assume $\Delta\hat{O}(\varphi) = \Delta\hat{O}(\varphi+\Delta\varphi)$.

The difference $\langle\hat{O}(\varphi+\delta\varphi)\rangle - \langle\hat{O}(\varphi)\rangle$ is experimentally detectable if

$$\langle\hat{O}(\varphi+\delta\varphi)\rangle - \langle\hat{O}(\varphi)\rangle \geqslant \Delta\hat{O}(\varphi), \tag{3}$$

where $\Delta\hat{O}(\varphi) := [\langle\hat{O}^2\rangle - \langle\hat{O}\rangle^2]^{1/2}$ is the standard deviation of $\hat{O}$. One can intuitively understand this condition graphically (see Fig. 1). The value of $\delta\varphi$ that saturates the inequality (3) is called sensitivity and is denoted by $\Delta\varphi$,

$$\Delta\varphi = \frac{\Delta\hat{O}}{\left|\frac{\partial}{\partial\varphi}\langle\hat{O}\rangle\right|}. \tag{4}$$

This equation will be pivotal in the following sections.

B. Transformations of the field operators

Consider a Mach-Zehnder interferometer composed of two mirrors $M_{1,2}$ and two balanced beam splitters $\mathrm{BS}_{1,2}$; the transmission (reflection) coefficient of $\mathrm{BS}_{1,2}$ is $T = 1/\sqrt{2}$ ($R = i/\sqrt{2}$) (see Fig. 2). We denote the two input (output) ports by 0 and 1 (4 and 5). The transformation of the field

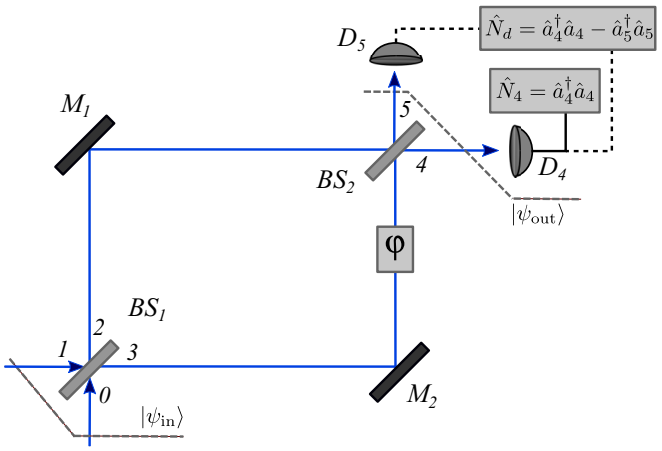

FIG. 2. Two detection schemes for the Mach-Zehnder interferometer we analyze here. The input state $|\psi_{\mathrm{in}}\rangle$ is unitarily transformed to the output $|\psi_{\mathrm{out}}\rangle$. The parameter we want to estimate via a suitable observable is the phase difference φ between the two arms of the MZI.

operators between the input and the output of the MZI is

$$\hat{a}_4^\dagger = -\sin\left(\frac{\varphi}{2}\right)\hat{a}_0^\dagger + \cos\left(\frac{\varphi}{2}\right)\hat{a}_1^\dagger,$$
$$\hat{a}_5^\dagger = \cos\left(\frac{\varphi}{2}\right)\hat{a}_0^\dagger + \sin\left(\frac{\varphi}{2}\right)\hat{a}_1^\dagger, \tag{5}$$

where we ignored global phases. We assume that the output ports 4 and 5 are connected to ideal detectors.

Usually the input state $|\psi_{\rm in}\rangle$ is given and we calculate either the output photocurrents or the difference between the output photocurrents. In the following we denote by φ the total phase shift inside the interferometer. The total phase has two parts: (i) the unknown (e.g., sensor-generated) phase shift φ_s, which is the quantity we want to measure, and (ii) the experimentally controllable part $\varphi_{\rm expt}$,

$$\varphi = \varphi_s + \varphi_{\rm expt}. \tag{6}$$

We assume that $|\varphi_s| \ll |\varphi|$, so in order to have the best performance, the experimenter must adjust $\varphi_{\rm expt}$ as close as possible to the optimal phase shift $\varphi^{\rm opt}$.

C. Output observables

Each detection scheme has an associated observable characterizing the measurement setup. We will discuss two measurement strategies: (i) the difference intensity detection scheme and (ii) the single-mode intensity detection scheme.

For Mach-Zehnder interferometers, a well-known approach of calculating the phase sensitivity is Schwinger's scheme based on angular momentum operators [4,34]. Although this method gives faster results for a difference intensity detector setup, it is not well suited for the single-mode intensity detection scheme we investigate here. Alternatively, one can use a Wigner-function-based method [29]. In this paper we use a brute-force calculation based on the field operator transformations (5).

1. Difference intensity detection scheme

In the first detection strategy we calculate the difference between the output photocurrents [i.e., detectors D_4 and D_5 (see Fig. 2)]. Thus, the observable conveying information about the phase φ is

$$\hat{N}_d(\varphi) = \hat{a}_4^\dagger\hat{a}_4 - \hat{a}_5^\dagger\hat{a}_5. \tag{7}$$

Using the field operator transformations (5), we have

$$\langle\hat{N}_d\rangle = \cos\varphi(\langle\hat{a}_1^\dagger\hat{a}_1\rangle - \langle\hat{a}_0^\dagger\hat{a}_0\rangle) - \sin\varphi(\langle\hat{a}_0\hat{a}_1^\dagger\rangle + \langle\hat{a}_0^\dagger\hat{a}_1\rangle), \tag{8}$$

where the expectation values are calculated with respect to the input state $|\psi_{\rm in}\rangle$. To estimate the phase sensitivity in Eq. (4) we need the absolute value of the derivative

$$\left|\frac{\partial\langle\hat{N}_d\rangle}{\partial\varphi}\right| = |\sin\varphi(\langle\hat{a}_0^\dagger\hat{a}_0\rangle - \langle\hat{a}_1^\dagger\hat{a}_1\rangle) - \cos\varphi(\langle\hat{a}_0\hat{a}_1^\dagger\rangle + \langle\hat{a}_0^\dagger\hat{a}_1\rangle)|. \tag{9}$$

In the following sections we will calculate this for various input states. The standard deviation $\Delta\hat{N}_d = [\langle\hat{N}_d^2\rangle - \langle\hat{N}_d\rangle^2]^{1/2}$ follows from Eq. (8) and Appendix B.

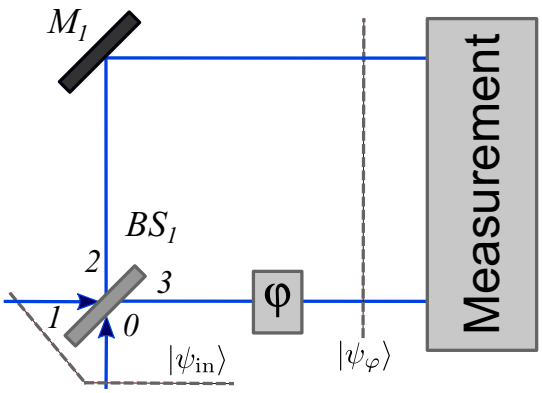

FIG. 3. In the Fisher information approach the Mach-Zehnder interferometer is considered up to the phase-shift operation [in our case $\hat{U}(\varphi) = e^{-i\varphi\hat{a}_3^\dagger\hat{a}_3}$] and the detection scheme completely disregarded; we have $|\psi_\varphi\rangle = \hat{U}(\varphi)\hat{U}_{\rm BS}|\psi_{\rm in}\rangle$, where $\hat{U}_{\rm BS}$ is the unitary corresponding to $\rm BS_1$.

2. Single-mode intensity detection scheme

We now consider the single-mode intensity detection scheme, i.e., we have only one detector coupled at the output port 4 (see Fig. 2). Thus the operator of interest is $\hat{N}_4 = \hat{a}_4^\dagger\hat{a}_4$. From Eq. (5) we have

$$\langle\hat{N}_4\rangle = \sin^2\left(\frac{\varphi}{2}\right)\langle\hat{a}_0^\dagger\hat{a}_0\rangle + \cos^2\left(\frac{\varphi}{2}\right)\langle\hat{a}_1^\dagger\hat{a}_1\rangle - \frac{\sin\varphi}{2}\langle\hat{a}_0\hat{a}_1^\dagger\rangle - \frac{\sin\varphi}{2}\langle\hat{a}_0^\dagger\hat{a}_1\rangle \tag{10}$$

and the absolute value of its derivative with respect to φ is

$$\left|\frac{\partial\langle\hat{N}_4\rangle}{\partial\varphi}\right| = \frac{1}{2}|\sin\varphi(\langle\hat{a}_0^\dagger\hat{a}_0\rangle - \langle\hat{a}_1^\dagger\hat{a}_1\rangle) - \cos\varphi(\langle\hat{a}_0\hat{a}_1^\dagger\rangle + \langle\hat{a}_0^\dagger\hat{a}_1\rangle)|. \tag{11}$$

As before, the standard deviation $\Delta\hat{N}_4$ follows from Eq. (10) and Appendix B.

D. Parameter estimation via Fisher information

The Fisher information is a very elegant approach of finding the best-case solution of parameter estimation [35]. The lower bound for the estimation of a parameter φ is given by the Cramér-Rao bound [4,27,36]

$$\Delta\varphi \geqslant \frac{1}{\sqrt{F(\varphi)}}, \tag{12}$$

where $F(\varphi)$ is the Fisher information. The Fisher information $F(\varphi)$ is maximized by the quantum Fisher information [35] $F(\varphi) \leqslant H(\varphi)$. This leads to the quantum Cramér-Rao bound (QCRB)

$$\Delta\varphi \geqslant \frac{1}{\sqrt{H(\varphi)}}. \tag{13}$$

Here $H(\varphi) = \mathrm{Tr}[\hat{\rho}_\varphi\hat{L}_\varphi^2]$ and $\hat{\rho}_\varphi = |\psi_\varphi\rangle\langle\psi_\varphi|$ is the density matrix of our system (see Fig. 3); $\hat{L}_\varphi$ is the symmetric logarithmic derivative defined as [4,35,36] $\hat{L}_\varphi\hat{\rho}_\varphi + \hat{\rho}_\varphi\hat{L}_\varphi = 2\partial\hat{\rho}_\varphi/\partial\varphi$. Moreover, if the system is in

a pure state the quantum Fisher information is $H(\varphi) = 4(\langle\partial_\varphi\psi_\varphi|\partial_\varphi\psi_\varphi\rangle - |\langle\partial_\varphi\psi_\varphi|\psi_\varphi\rangle|^2)$, where $|\partial_\varphi\psi_\varphi\rangle = \partial|\psi_\varphi\rangle/\partial\varphi$ [26,27,36].

Importantly, calculating the Fisher information for a given scenario is not always straightforward and moreover it can lead to different results [37]. Indeed, an external phase reference is needed with respect to what are defined as the two phase shifts, each in one arm of the MZI. For this reason, a two-parameter estimation problem involving a Fisher matrix is used [24] (see Appendix A). When an external phase reference is not available, one has to pay particular attention to what is actually measurable given the experimental setup [38].

We stress that in the evaluation of the QCRB the detection scheme is disregarded (see Fig. 3). The QCRB will always be a theoretical best-case scenario, which overlooks practical implementations of the detection stage. In the following, for each case discussed in Secs. III–V we will compare the practically achievable results with the QCRB from Eq. (13).

III. SINGLE COHERENT INPUT

In this section we consider the input port 1 in a coherent state $|\alpha\rangle$ while input port 0 is kept "dark" (i.e., in the vacuum state). The input state is

$$|\psi_{\text{in}}\rangle = |\alpha_1 0_0\rangle = \hat{D}_1(\alpha)|0\rangle, \tag{14}$$

where $\hat{D}_1(\alpha) = e^{\alpha\hat{a}_1^\dagger - \alpha^*\hat{a}_1}$ is the displacement operator [6,7,10].

A. Difference intensity detection scheme

The observable we measure is the difference in the photocurrents at the outputs 4 and 5, namely, the average value of $\hat{N}_d$ [Eq. (7)]. For the input state (14) we find $\langle\hat{N}_d\rangle = \cos\varphi|\alpha|^2$ and, using Eq. (B1), the output variance is found to be $\Delta^2\hat{N}_d = |\alpha|^2$. Consequently, the phase sensitivity of a Mach-Zehnder interferometer driven by a single coherent source is

$$\Delta\varphi_{\text{diff}} = \frac{1}{|\sin\varphi||\alpha|} = \frac{1}{|\sin\varphi|\sqrt{\langle N\rangle}}, \tag{15}$$

where the average number of photons is $\langle N\rangle = |\alpha|^2$ and this is the well-known shot-noise limit or standard quantum limit [4,28].

B. Single-mode intensity detection scheme

In a single-mode intensity detection setup the average of the output observable $\hat{N}_4$ gives

$$\langle\hat{N}_4\rangle = \cos^2\left(\frac{\varphi}{2}\right)|\alpha|^2. \tag{16}$$

The variance of $\hat{N}_4$ follows from Eqs. (B2) and (16), giving $\Delta^2\hat{N}_4 = \cos^2(\varphi/2)|\alpha|^2$. Thus, the phase sensitivity in the single-mode intensity detection case is

$$\Delta\varphi_{\text{sing}} = \frac{1}{\left|\sin\left(\frac{\varphi}{2}\right)\right||\alpha|} = \frac{1}{\left|\sin\left(\frac{\varphi}{2}\right)\right|\sqrt{\langle N\rangle}}. \tag{17}$$

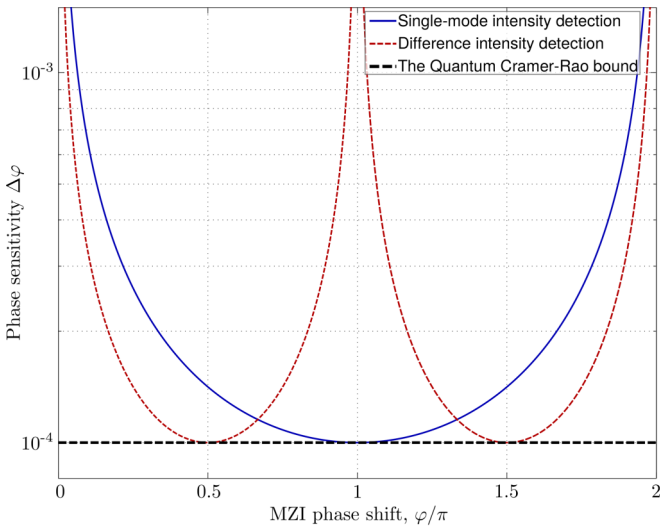

FIG. 4. Phase sensitivity for the single-mode (solid blue line) and difference (dashed red line) intensity detection setups compared to the quantum Cramér-Rao bound (thick dashed line) for a single coherent input with $|\alpha| = 10^4$. Both configurations reach the Cramér-Rao bound at their respective optimal phase shifts.

C. Discussion: The quantum Cramér-Rao bound

For a single input coherent state, the QCRB in Eq. (13) is [4,37]

$$\Delta\varphi_{\text{QCRB}} \geqslant \frac{1}{|\alpha|} = \frac{1}{\sqrt{\langle N\rangle}}. \tag{18}$$

Both detection schemes reach this limit, but at different values of the total internal phase shift, as depicted in Fig. 4.

In the differential detection scheme, the optimal sensitivity is reached for $|\sin\varphi| = 1$, i.e., $\varphi_{\text{diff}}^{\text{opt}} = \pi/2 + k\pi$, $k \in \mathbb{Z}$ [see Eq. (15)]. This implies equal output power at the two outputs (4 and 5). There is no dark port in the case of the difference intensity detection. This can be a major drawback if one uses a high input power in order to lower the sensitivity.

For single-mode intensity detection, the phase sensitivity (17) reaches the QCRB at $\varphi_{\text{sing}}^{\text{opt}} = \pi + 2k\pi$, $k \in \mathbb{Z}$ (see Fig. 4). This means that the output 4 is a dark port. This is a clear advantage for high input power since we can use extremely sensitive *p-i-n* photodiodes [39].

IV. DOUBLE COHERENT INPUT

An interesting situation arises if we apply a coherent source in each input port of the interferometer

$$|\psi_{\text{in}}\rangle = |\alpha_1\beta_0\rangle = \hat{D}_1(\alpha)\hat{D}_0(\beta)|0\rangle, \tag{19}$$

where the displacement operator at input port 0 is $\hat{D}_0(\beta) = e^{\beta\hat{a}_0^\dagger - \beta^*\hat{a}_0}$. Here $\alpha = |\alpha|e^{i\theta_\alpha}$, $\beta = |\beta|e^{i\theta_\beta}$, and $\Delta\theta = \theta_\alpha - \theta_\beta$ is the phase difference between the two input lasers.

A. Differential detection scheme

Using the input state given in Eq. (19), the average value of the operator $\hat{N}_d$ is

$$\langle\hat{N}_d\rangle = \cos\varphi(|\alpha|^2 - |\beta|^2) - 2\sin\varphi|\alpha\beta|\cos\Delta\theta. \tag{20}$$

After a straightforward computation, the variance is

$$\Delta^2 \hat{N}_d^2 = |\alpha|^2 + |\beta|^2 = |\alpha|^2(1+\varpi^2), \tag{21}$$

where $\varpi := |\beta|/|\alpha|$. The phase sensitivity for a double coherent input is

$$\Delta\varphi_{\text{diff}} = \frac{\sqrt{1+\varpi^2}}{|\alpha||\sin\varphi(1-\varpi^2) + 2\cos\varphi\varpi\cos\Delta\theta|}. \tag{22}$$

We will discuss this result in Sec. IV C.

B. Single-mode intensity detection scheme

In the single-mode intensity detection setup, the average of our output observable is

$$\langle \hat{N}_4 \rangle = |\alpha|^2\left[\sin^2\left(\frac{\varphi}{2}\right)\varpi^2 + \cos^2\left(\frac{\varphi}{2}\right) - \sin\varphi\varpi\cos\Delta\theta\right]. \tag{23}$$

The variance $\Delta^2\hat{N}_4$ can be computed as before; alternatively, we notice that at the output port 4 we have a coherent state, therefore the variance is equal to its average value

$$\Delta^2\hat{N}_4 = \langle \hat{N}_4 \rangle \tag{24}$$

Thus, the phase sensitivity of a Mach-Zehnder with two input coherent sources and a single-mode intensity detection scheme is

$$\Delta\varphi_{\text{sing}} = \frac{\sqrt{\sin^2\left(\frac{\varphi}{2}\right)\varpi^2 + \cos^2\left(\frac{\varphi}{2}\right) - \sin\varphi\varpi\cos\Delta\theta}}{|\alpha|\left|\frac{\sin\varphi}{2}(1-\varpi^2) + \cos\varphi\varpi\cos\Delta\theta\right|}. \tag{25}$$

C. Discussion: The quantum Cramér-Rao bound

For the double coherent input, the quantum Cramér-Rao bound is (see Appendix A)

$$\Delta\varphi_{\text{QCRB}} \geqslant \frac{1}{|\alpha|\sqrt{1+\varpi^2 - \frac{4\varpi^2}{1+\varpi^2}\sin^2\Delta\theta}}. \tag{26}$$

Therefore, the best sensitivity is achieved when the two input lasers are in phase, $\Delta\theta = 0$, resulting in $\Delta\varphi_{\text{QCRB}} = 1/(|\alpha|\sqrt{1+\varpi^2})$.

In the case of differential detection, one can show that an optimum phase shift exists,

$$\varphi_{\text{diff}}^{\text{opt}} = \pm\arctan\left(\frac{|1-\varpi^2|}{2\varpi|\cos\Delta\theta|}\right) + k\pi, \tag{27}$$

where $k \in \mathbb{Z}$ and $\varphi_{\text{diff}}^{\text{opt}}$ brings the sensitivity from Eq. (22) to the QCRB. For the single-mode intensity detection scheme, if the two input lasers are in phase ($\Delta\theta = 0$), the optimum phase shift is

$$\varphi_{\text{sing}}^{\text{opt}} = \pm 2\arctan\left(\frac{1}{\varpi}\right) + 2k\pi, \tag{28}$$

where $k \in \mathbb{Z}$ and substituting this value into Eq. (25) gives the QCRB from Eq. (26).

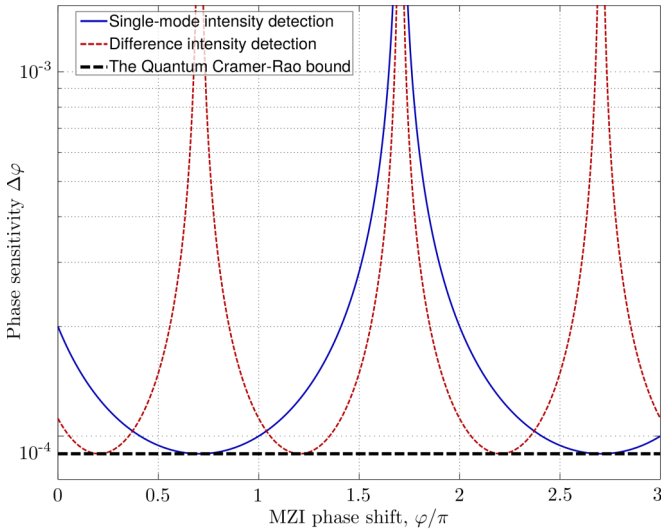

FIG. 5. Phase sensitivity for the single-mode intensity (solid blue line) and difference intensity (dashed red line) detection setups versus the phase shift φ. Both detection schemes reach the quantum Cramér-Rao bound (thick dashed line). We used the parameters $|\alpha| = 10^4$, $\varpi = 0.5$, and $\Delta\theta = 0$.

For comparison, the sensitivity of homodyne detection with $\Delta\theta = 0$ is

$$\Delta\varphi_H \geqslant \frac{1}{\left|\alpha\sin\frac{\varphi}{2} + \beta\cos\frac{\varphi}{2}\right|}. \tag{29}$$

The phase sensitivity of a MZI with a double coherent input is shown in Fig. 5 for both single-mode and difference intensity detection schemes. As already discussed, we can reach the QCRB in both scenarios.

Compared to the single coherent input, the double coherent case has an important advantage: We can tune the value of $\varphi_{\text{sing}}^{\text{opt}}$ at which the sensitivity reaches the QCRB. Experimentally, this can be achieved by varying the power ratio of the two input coherent sources. This avoids the use of piezoelectricity or other mechanical-based methods to induce phase shifts. As a consequence, our proposal reduces mechanical vibrations, noise, or misalignments.

In the high-power regime this ability is practically useful for a single-mode intensity detection scenario. Indeed, at the optimal phase shift the output 4 is a dark port, i.e., $\langle \hat{N}_4(\varphi_{\text{sing}}^{\text{opt}})\rangle \to 0$, which is exactly the desired situation with respect to the photodetectors in the high-power regime.

V. COHERENT PLUS SQUEEZED VACUUM INPUT

The paradigmatic input state which beats the SQL is the coherent plus squeezed vacuum

$$|\psi_{\text{in}}\rangle = |\alpha_1 r_0\rangle = D_1(\alpha)S_0(r)|0\rangle. \tag{30}$$

The squeezed vacuum state is obtained by applying the squeezing operator $S_0(\xi) = e^{[(\xi^*)^2\hat{a}_1^2 - \xi^2(\hat{a}_1^\dagger)^2]/2}$ [6,8,10] with $\xi = re^{i\theta}$. For simplicity, in the following we take $\theta = 0$, hence $\xi = r \in \mathbb{R}^+$. This input state is of considerable practical interest as it was shown to beat the SQL [2,11,12,24,25], a prediction amply confirmed by experiments [3,13,14,40].

A. Difference intensity detection scheme

With the coherent plus squeezed vacuum input (30) the average of $\hat{N}_d$ in Eq. (7) is

$$\langle \hat{N}_d \rangle = \cos\varphi(|\alpha|^2 - \sinh^2 r). \tag{31}$$

The variance $\Delta^2 \hat{N}_d$ can be computed using Eqs. (7) and (B1), with the input state given in (30), and yields

$$\Delta^2 \hat{N}_d = \cos^2\varphi\left(\frac{\sinh^2 2r}{2} + |\alpha|^2\right) + \sin^2\varphi(\sinh^2 r + |\alpha|^2 e^{-r}) + \sin^2\varphi|\alpha|^2 \sinh 2r(1-\cos 2\theta_\alpha). \tag{32}$$

For the difference intensity detection scheme, the best achievable phase sensitivity of a MZI with coherent plus squeezed vacuum input is

$$\Delta\varphi_{\text{diff}} = \frac{\sqrt{\left(|\alpha|^2 + \frac{\sinh^2 2r}{2}\right)\cot^2\varphi + \sinh^2 r + |\alpha|^2 e^{-2r} + |\alpha|^2 \sinh 2r(1-\cos 2\theta_\alpha)}}{|\sinh^2 r - |\alpha|^2|}. \tag{33}$$

The last term in the numerator of Eq. (33) is the input noise enhancement due to the misalignment of the coherent input with respect to the squeezed vacuum (whose phase we considered to be zero, for simplicity). The best sensitivity is achieved for $\theta_\alpha = 0$ (hence $\alpha \in \mathbb{R}$),

$$\Delta\varphi_{\text{diff}} = \frac{\sqrt{\left(\alpha^2 + \frac{\sinh^2 2r}{2}\right)\cot^2\varphi + \sinh^2 r + \alpha^2 e^{-2r}}}{|\alpha^2 - \sinh^2 r|}, \tag{34}$$

an expression that can be found in the literature [4,23].

B. Single-mode intensity detection scheme

For the input state (30) we have

$$\langle \hat{N}_4 \rangle = \sin^2\left(\frac{\varphi}{2}\right)\sinh^2 r + \cos^2\left(\frac{\varphi}{2}\right)|\alpha|^2 \tag{35}$$

and the variance is

$$\begin{aligned}\Delta^2 \hat{N}_4 = {} & \sin^4\left(\frac{\varphi}{2}\right)\frac{\sinh^2 2r}{2} + \sin^2\left(\frac{\varphi}{2}\right)\cos^2\left(\frac{\varphi}{2}\right)\sinh^2 r + \cos^4\left(\frac{\varphi}{2}\right)|\alpha|^2 \\ & + \sin^2\left(\frac{\varphi}{2}\right)\cos^2\left(\frac{\varphi}{2}\right)|\alpha|^2 e^{-2r} + \frac{\sin^2\varphi}{4}\sinh 2r|\alpha|^2(1-\cos 2\theta_\alpha).\end{aligned} \tag{36}$$

In the single-mode intensity detection setup, the best achievable sensitivity of a MZI fed by coherent plus squeezed vacuum input is

$$\Delta\varphi_{\text{sing}} = \frac{\sqrt{\frac{\tan^2\left(\frac{\varphi}{2}\right)\sinh^2 2r}{2} + \sinh^2 r + \frac{|\alpha|^2}{\tan^2\left(\frac{\varphi}{2}\right)} + |\alpha|^2 e^{-2r} + \sinh 2r|\alpha|^2(1-\cos 2\theta_\alpha)}}{||\alpha|^2 - \sinh^2 r|}. \tag{37}$$

The last term of the square root is again the contribution of the misalignment of the coherent input from port 1 with the squeezed vacuum from port 0. The best sensitivity is obtained for $\cos 2\theta_\alpha = 1$, thus $\theta_\alpha = 0$ and hence $\alpha \in \mathbb{R}$. Therefore, we have now the best achievable sensitivity for the squeezed plus coherent input and a single-mode intensity detection scheme [33]

$$\Delta\varphi_{\text{sing}} = \frac{\sqrt{\frac{\tan^2\left(\frac{\varphi}{2}\right)\sinh^2 2r}{2} + \sinh^2 r + \frac{\alpha^2}{\tan^2\left(\frac{\varphi}{2}\right)} + \alpha^2 e^{-2r}}}{|\alpha^2 - \sinh^2 r|}. \tag{38}$$

C. Discussion: The quantum Cramér-Rao bound

The quantum Cramér-Rao bound for the coherent plus squeezed vacuum input is [23–25,37]

$$\Delta\varphi_{\text{QCRB}} \geqslant \frac{1}{\sqrt{|\alpha|^2 e^{2r} + \sinh^2 r}} \tag{39}$$

and is independent of the phase shift φ of the MZI, similar to the coherent input case. For comparison, we briefly mention the sensitivity of the homodyne detection scheme [29,41]

$$\Delta\varphi_H \geqslant \frac{e^{-r}}{|\alpha|}, \tag{40}$$

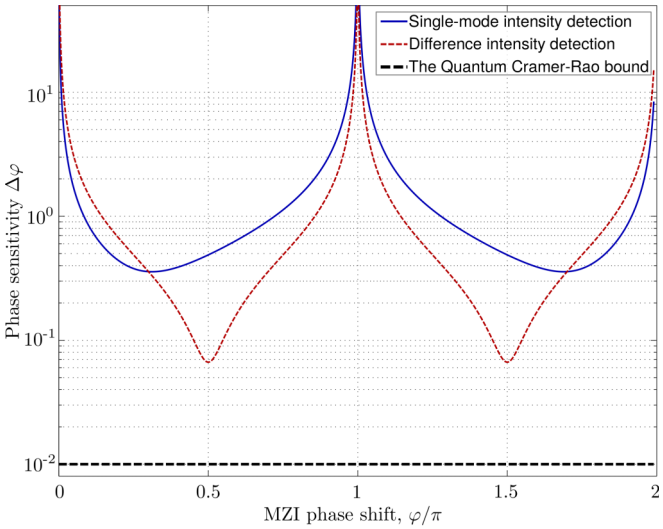

FIG. 6. Phase sensitivity for the single-mode (solid blue line) and difference (dashed red line) intensity detection setups compared to the quantum Cramér-Rao bound (thick dashed line) versus the phase shift φ. Here $|\alpha| = 10$ and $r = 2.3$.

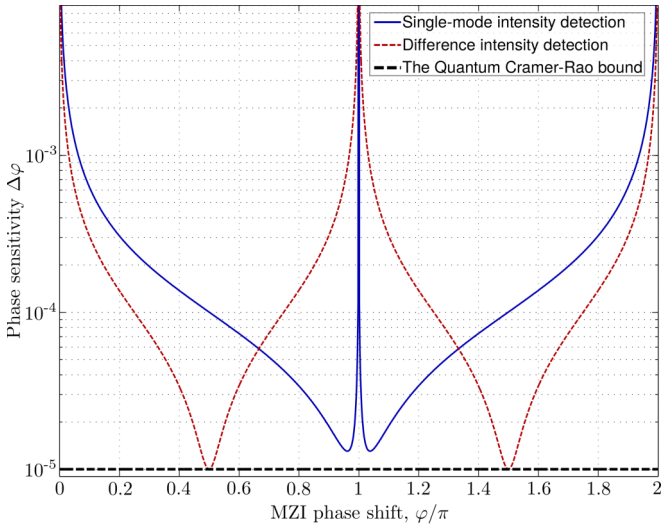

FIG. 7. Phase sensitivity for the single-mode (solid blue line) and difference (dashed red line) intensity detection setups compared to the quantum Cramér-Rao bound (thick dashed line) versus the phase shift φ. We use $|\alpha| = 10^4$ and $r = 2.3$.

a result we will use later. For the differential detection scheme, the optimal sensitivity in Eq. (34) is reached for $\cos\varphi = 0$, i.e., $\varphi_{\rm diff}^{\rm opt} = \pi/2 + k\pi$, $k \in \mathbb{Z}$, and we find the best achievable sensitivity

$$\Delta\varphi_{\rm diff} = \frac{\sqrt{\sinh^2 r + \alpha^2 e^{-2r}}}{|\alpha^2 - \sinh^2 r|}, \tag{41}$$

a result also found in the literature [4,23,29]. For single-mode intensity detection, the optimal sensitivity from Eq. (38) is reached when

$$\varphi_{\rm sing}^{\rm opt} = \pm 2 \arctan\left(\sqrt{\frac{\sqrt{2}|\alpha|}{\sinh 2r}}\right) + 2k\pi \tag{42}$$

with $k \in \mathbb{Z}$; substituting this value in equation (38) gives the best achievable sensitivity in the case of a single-mode intensity scheme, namely,

$$\Delta\varphi_{\rm sing} = \frac{\sqrt{\sinh^2 r + \sqrt{2}\alpha \sinh 2r + \alpha^2 e^{-2r}}}{|\alpha^2 - \sinh^2 r|}. \tag{43}$$

This result is identical to the one reported in Ref. [29], Eq. (10).

In Figs. 6 and 7 we plot the best achievable phase sensitivity in the single-mode and difference intensity detection schemes together with the Cramér-Rao bound from Eq. (39) for coherent plus squeezed vacuum input versus the phase shift of the MZI. One notes that both detection schemes have an optimum, however neither reaches the QCRB. (Although in Fig. 7 it seems that the red curve corresponding to the difference intensity detection scenario reaches the QCRB, it actually stays above it.) While the optimum working point for the difference intensity detection scheme is constant, in the transition from the low- (Fig. 6) to the high-power regime (Fig. 7) the optimum working point $\varphi^{\rm opt}$ shifts [see Eq. (43)].

In Fig. 8 we show both $\Delta\varphi_{\rm diff}$ and $\Delta\varphi_{\rm sing}$ in the low-$|\alpha|$ regime. For $|\alpha|^2 \approx \sinh^2 r$ both detection schemes give poor results while the QCRB reaches the Heisenberg limit $\Delta\varphi_{\rm QCRB} \sim 1/\langle N\rangle$, where $\langle N\rangle = |\alpha|^2 + \sinh^2 r$. This behavior has been explained by Pezzé and Smerzi [23] and was attributed to the limited information gained by these phase estimation techniques, notably due to the ignorance of the fluctuation in the number of particles.

Ideally one would like to enhance the squeezing factor r as much as possible. However, this is experimentally challenging [16,17,40]. The maximum reported squeezing was 15 dB, corresponding to $r \approx 2.3$ [17]. Therefore, in order to remain

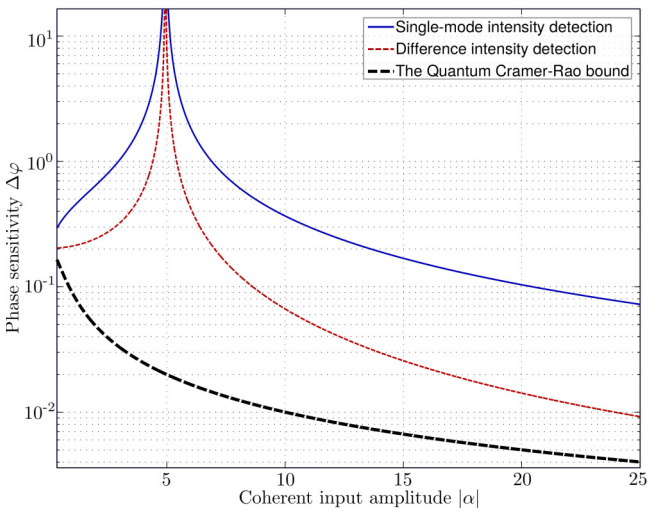

FIG. 8. Phase sensitivity for the single-mode (solid blue line) and difference (dashed red line) intensity detection schemes and the quantum Cramér-Rao bound (thick dashed line) versus the coherent input amplitude $|\alpha|$, in the low-intensity regime. We take the squeezing factor $r = 2.3$ and consider the optimal phases $\varphi^{\rm opt}$ for each detection scenario. Both detection techniques are suboptimal with respect to the QCRB, yielding poor performance especially when $|\alpha|^2 \approx \sinh^2 r$.

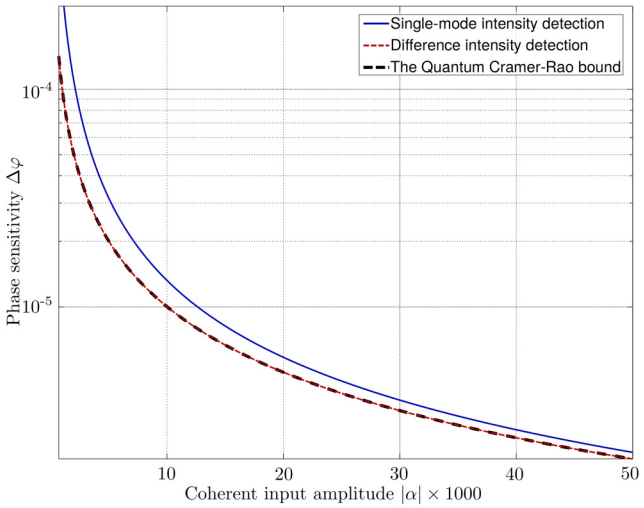

FIG. 9. Phase sensitivity for the single-mode (solid blue line) and difference (dashed red line) intensity detection schemes and the quantum Cramér-Rao bound (thick dashed line) versus the coherent input amplitude $|\alpha|$, in the high-intensity regime. We consider a squeezing factor $r = 2.3$ and we plot the optimal phases for each detection scenario. As $|\alpha|$ grows, both detection schemes approach the Cramér-Rao bound.

realistic in the high-intensity regime, we keep r constant and small compared to the amplitude of the coherent state, implying $|\alpha|^2 \gg |\alpha| \gg \sinh^2 r$. Indeed, for $|\alpha| \gg \sinh r$ both detection schemes equal the sensitivity of the homodyne detection in Eq. (40). The QCRB in Eq. (39) can be approximated by $\Delta\varphi \approx e^{-r}/|\alpha|$. Thus, using squeezing in port 0 brings a factor of e^{-r} over the SQL, therefore the coherent plus squeezed vacuum technique remains interesting even for large $|\alpha|$.

In Fig. 9 we plot both $\Delta\varphi_{\rm diff}$ and $\Delta\varphi_{\rm sing}$ in the high-$|\alpha|$ regime. We conclude that if $|\alpha|^2 \gg |\alpha| \gg \sinh r$, both detection schemes have a similar sensitivity, close to the QCRB. This agrees with the results of Ref. [29].

As already mentioned, the optimum phase shift inside the Mach-Zehnder interferometer for a difference intensity detection scheme is constant, $\varphi_{\rm diff}^{\rm opt} = \pi/2 + k\pi$. In this case each output port receives roughly half of the (large) input power; this regime is clearly not desirable for the detectors.

For a single-mode intensity detection scheme, $\varphi_{\rm sing}^{\rm opt}$ is given by Eq. (42). Moreover, in this scenario port 4 is almost dark and consequently we can use extremely sensitive *p-i-n* photodiodes. Almost all power exits through the output 5 and can be discarded or used for a feedback loop to stabilize the input laser. This is the crucial difference between the two schemes in the high-intensity regime, similarly to the single and double coherent input cases (see Secs. III and IV).

In this paper we did not consider losses or decoherence. The impact of losses on various scenarios has been discussed extensively in the literature [29,42–44]. In the following we briefly discuss their effect in the high-intensity regime. Following [43], in the case of a coherent input we can replace $\alpha \to \alpha\sqrt{1-\sigma}$, resulting in a quantum Cramér-Rao bound $\Delta\varphi_{\rm QCRB} = 1/|\alpha|\sqrt{1-\sigma}$. The effect of small losses ($\sigma \ll 1$) is marginal for a coherent source. In the case of coherent plus squeezed vacuum input we have [43] the Cramér-Rao bound

$$\Delta\varphi_{\rm QCRB}^{\rm loss} \approx \frac{\sqrt{\sigma + (1-\sigma)e^{-2r}}}{\sqrt{(1-\sigma)|\alpha|^2 + \sigma(1-\sigma)\sinh^2 r}}. \tag{44}$$

The effect of losses is obvious for high squeezing factors, the numerator of Eq. (44) being reduced to $\sqrt{\sigma}$, thus losing the exponential factor from the squeezing of the input vacuum. Nonetheless, for the high-intensity regime discussed in this paper we have $|\alpha|/\sinh r \gg 1$ and the effect of small losses is rather limited because $\sigma \ll (1-\sigma)e^{-2r}$. For simplicity, we did not consider the $1/\sqrt{m}$ scaling for all phase sensitivities throughout this paper, where m is the number of repeated experiments. We summarized our results in Table I.

VI. CONCLUSIONS

The sensitivity of a Mach-Zehnder interferometer depends on both the input state and the detection setup. To achieve the best sensitivity we need to find the optimum working point(s) of the interferometer.

For single coherent and double coherent input, both detection setups achieve the QCRB, although at different values of φ. The double coherent input allows us to experimentally tune the point of maximum sensitivity by adjusting the relative intensity of the two coherent states. This is an advantage over other methods involving mechanically adjusted setups.

In the high-intensity regime all three input states (coherent, double coherent, and coherent plus squeezed vacuum)

TABLE I. Phase sensitivity of a MZI for the input states discussed in the paper. The optimum phase shift has a period of π for the difference intensity detection and 2π for the single-mode intensity detection.

Input state $\lvert\psi_{\rm in}\rangle$	Quantum Cramér-Rao bound $\Delta\varphi_{\rm QCRB}$	Difference intensity detection: Optimum phase shift $\varphi_{\rm diff}^{\rm opt}$	Difference intensity detection: Best achievable phase sensitivity $\Delta\varphi_{\rm diff}(\varphi_{\rm diff}^{\rm opt})$	Single-mode intensity detection: Optimum phase shift $\varphi_{\rm sing}^{\rm opt}$	Single-mode intensity detection: Best achievable phase sensitivity $\Delta\varphi_{\rm sing}(\varphi_{\rm sing}^{\rm opt})$
$\lvert\alpha_1\rangle$	$\frac{1}{\lvert\alpha\rvert}$	$\frac{\pi}{2}$	$\frac{1}{\lvert\alpha\rvert}$	π	$\frac{1}{\lvert\alpha\rvert}$
$\lvert\alpha_1\beta_0\rangle$	$\frac{\sqrt{1+\varpi^2}}{\lvert\alpha\rvert\sqrt{(1+\varpi^2)^2-2\varpi\sin^2\Delta\theta}}$	$\pm\arctan\left(\frac{1-\varpi^2}{2\varpi}\right)$	$\Delta\varphi_{\rm QCRB}$	$\pm 2\arctan\left(\frac{1}{\varpi}\right)$	$\Delta\varphi_{\rm QCRB}$
$\lvert\alpha_1\xi_0\rangle$	$\frac{1}{\sqrt{\lvert\alpha\rvert^2 e^{2r}+\sinh^2 r}}$	$\frac{\pi}{2}$	$\frac{\sqrt{\sinh^2 r+\alpha^2 e^{-2r}}}{\lvert\alpha^2-\sinh^2 r\rvert}$	$\pm 2\arctan\left(\sqrt{\frac{\sqrt{2}\lvert\alpha\rvert}{\sinh r}}\right)$	$\frac{\sqrt{\sinh^2 r+\sqrt{2}\alpha\sinh 2r+\alpha^2 e^{-2r}}}{\lvert\alpha^2-\sinh^2 r\rvert}$

give similar phase sensitivity, at or close to the QCRB. The optimum working point for the single-mode intensity detection has an almost dark output port. This ensures that one can use highly efficient *p-i-n* photodiodes and thus avoid potential problems of overheating or blinding the photodetectors. We expect that our results will lead to more sensitive detection systems for interferometry in the high-power regime.

ACKNOWLEDGMENTS

S.A. acknowledges support from Extreme Light Infrastructure–Nuclear Physics Phase II, a project cofinanced by the Romanian Government and the European Union through the European Regional Development Fund and the Competitiveness Operational Program (1/07.07.2016, COP, ID 1334). R.I. acknowledges support from a grant of the Romanian Ministry of Research and Innovation, PCCDI-UEFISCDI, Project No. PN-III-P1-1.2-PCCDI-2017-0338/79PCCDI/2018, within PNCDI III and PN 18090101/2018.

APPENDIX A: QUANTUM CRAMÉR-RAO BOUND FOR A DOUBLE COHERENT INPUT

Following Ref. [24], we consider the general case where each arm of the MZI contains a phase shift (φ_1 and φ_2). The estimation is treated as a general two-parameter problem. We define the 2×2 Fisher information matrix

$$\mathcal{F} = \begin{bmatrix} \mathcal{F}_{++} & \mathcal{F}_{+-} \\ \mathcal{F}_{-+} & \mathcal{F}_{--} \end{bmatrix}, \tag{A1}$$

where

$$\mathcal{F}_{ij} = 4\,\mathrm{Re}(\langle\partial_i\psi|\partial_j\psi\rangle - \langle\partial_i\psi|\psi\rangle\langle\psi|\partial_j\psi\rangle), \tag{A2}$$

with $i, j = \pm$ and $\varphi_\pm = \varphi_1 \pm \varphi_2$. From this matrix we can easily compute the QCRB

$$\langle\Delta\varphi_i\Delta\varphi_j\rangle \geqslant (\mathcal{F}^{-1})_{ij}. \tag{A3}$$

The state $|\psi\rangle$ in Eq. (A2) is

$$|\psi\rangle = e^{-i(\varphi_+/2)(a_2^\dagger a_2 + a_3^\dagger a_3)} e^{-i(\varphi_-/2)(a_2^\dagger a_2 - a_3^\dagger a_3)} |\psi_{23}\rangle, \tag{A4}$$

where $|\psi_{23}\rangle = U_{\mathrm{BS}}|\alpha_1\beta_0\rangle$ is the state after the first beam splitter and $U_{\mathrm{BS}} = e^{-i\pi/4(\hat{a}_0^\dagger\hat{a}_0 + \hat{a}_1^\dagger\hat{a}_1)}$ is the unitary transformation of BS_1. The elements of $\mathcal{F}$ are $\mathcal{F}_{++} = |\alpha|^2 + |\beta|^2$, $\mathcal{F}_{+-} = \mathcal{F}_{-+} = -2|\alpha\beta|\sin\Delta\theta$, and $\mathcal{F}_{--} = |\alpha|^2 + |\beta|^2$. We are interested in the phase difference between the two arms, i.e., $\langle(\Delta\varphi_-)^2\rangle \geqslant (\mathcal{F}^{-1})_{--}$, for which we obtain the QCRB

$$\Delta\varphi_{\mathrm{QCRB}} \geqslant \frac{1}{\sqrt{|\alpha|^2 + |\beta|^2 - \frac{4|\alpha\beta|^2\sin^2\Delta\theta}{|\alpha|^2+|\beta|^2}}}, \tag{A5}$$

which is equivalent to Eq. (26) with $\varpi = |\beta|/|\alpha|$.

APPENDIX B: CALCULATION OF THE OUTPUT VARIANCE

Here we compute the averages $\langle\hat{N}^2\rangle$ needed in the paper. For a difference intensity detection scheme, from Eqs. (7) and (5) we obtain the expression of $\hat{N}_d^2$ as a function of input operators $a_0^\dagger$ and $a_1^\dagger$. After a long but straightforward calculation we obtain the final, normally ordered expression

$$\begin{aligned}\langle\hat{N}_d^2\rangle = {} & \cos^2\varphi\langle\hat{a}_0^\dagger\hat{a}_0^\dagger\hat{a}_0\hat{a}_0\rangle - 2\cos(2\varphi)\langle\hat{a}_0^\dagger\hat{a}_0\hat{a}_1^\dagger\hat{a}_1\rangle + \cos^2\varphi\langle\hat{a}_1^\dagger\hat{a}_1^\dagger\hat{a}_1\hat{a}_1\rangle + \langle\hat{a}_0^\dagger\hat{a}_0\rangle + \langle\hat{a}_1^\dagger\hat{a}_1\rangle + \sin^2\varphi\langle\hat{a}_0^2(\hat{a}_1^\dagger)^2\rangle \\ & + \sin^2\varphi\langle(\hat{a}_0^\dagger)^2\hat{a}_1^2\rangle + \sin 2\varphi\langle\hat{a}_0^\dagger\hat{a}_0^2\hat{a}_1^\dagger\rangle + \sin 2\varphi\langle(\hat{a}_0^\dagger)^2\hat{a}_0\hat{a}_1\rangle - \sin 2\varphi\langle\hat{a}_0(\hat{a}_1^\dagger)^2\hat{a}_1\rangle - \sin 2\varphi\langle\hat{a}_0^\dagger\hat{a}_1^\dagger\hat{a}_1^2\rangle.\end{aligned} \tag{B1}$$

For the single-mode intensity detection setup, the calculation of $\langle\hat{N}_4^2\rangle$ is similar and we obtain

$$\begin{aligned}\langle\hat{N}_4^2\rangle = {} & \sin^4\left(\frac{\varphi}{2}\right)\langle\hat{a}_0^\dagger\hat{a}_0^\dagger\hat{a}_0\hat{a}_0\rangle + \cos^4\left(\frac{\varphi}{2}\right)\langle\hat{a}_1^\dagger\hat{a}_1^\dagger\hat{a}_1\hat{a}_1\rangle + \sin^2\varphi\langle\hat{a}_0^\dagger\hat{a}_0\hat{a}_1^\dagger\hat{a}_1\rangle + \sin^2\left(\frac{\varphi}{2}\right)\langle\hat{a}_0^\dagger\hat{a}_0\rangle + \cos^2\left(\frac{\varphi}{2}\right)\langle\hat{a}_1^\dagger\hat{a}_1\rangle \\ & + \frac{\sin^2\varphi}{4}\langle\hat{a}_0^2(\hat{a}_1^\dagger)^2\rangle + \frac{\sin^2\varphi}{4}\langle(\hat{a}_0^\dagger)^2\hat{a}_1^2\rangle - \sin^2\left(\frac{\varphi}{2}\right)\sin\varphi\langle\hat{a}_0^\dagger\hat{a}_0^2\hat{a}_1^\dagger\rangle - \sin^2\left(\frac{\varphi}{2}\right)\sin\varphi\langle(\hat{a}_0^\dagger)^2\hat{a}_0\hat{a}_1\rangle \\ & - \cos^2\left(\frac{\varphi}{2}\right)\sin\varphi\langle\hat{a}_0(\hat{a}_1^\dagger)^2\hat{a}_1\rangle - \cos^2\left(\frac{\varphi}{2}\right)\sin\varphi\langle\hat{a}_0^\dagger\hat{a}_1^\dagger\hat{a}_1^2\rangle - \frac{\sin\varphi}{2}\langle\hat{a}_0\hat{a}_1^\dagger\rangle - \frac{\sin\varphi}{2}\langle\hat{a}_0^\dagger\hat{a}_1\rangle.\end{aligned} \tag{B2}$$

[1] S. Barnett, C. Fabre, and A. Maıtre, Eur. Phys. J. D **22**, 513 (2003).
[2] C. M. Caves, Phys. Rev. D **23**, 1693 (1981).
[3] The LIGO Scientific Collaboration, Nat. Phys. **7**, 962 (2011).
[4] R. Demkowicz-Dobrzański, M. Jarzyna, and J. Kołodyński, Prog. Opt. **60**, 345 (2015).
[5] Y. Gao and H. Lee, Eur. Phys. J. D **68**, 347 (2014).
[6] C. Gerry and P. Knight, *Introductory Quantum Optics* (Cambridge University Press, Cambridge, 2005).
[7] L. Mandel and E. Wolf, *Optical Coherence and Quantum Optics* (Cambridge University Press, Cambridge, 1995).
[8] H. P. Yuen, Phys. Rev. A **13**, 2226 (1976).
[9] B. Yurke, Phys. Rev. A **32**, 300 (1985).
[10] G. S. Agarwal, *Quantum Optics* (Cambridge University Press, Cambridge, 2012).
[11] M. J. Holland and K. Burnett, Phys. Rev. Lett. **71**, 1355 (1993).
[12] M. G. Paris, Phys. Lett. A **201**, 132 (1995).
[13] J. Aasi *et al.*, Nat. Photon. **7**, 613 (2013).
[14] M. Xiao, L.-A. Wu, and H. J. Kimble, Phys. Rev. Lett. **59**, 278 (1987).
[15] G. Breitenbach, F. Illuminati, S. Schiller, and J. Mlynek, Europhys. Lett. **44**, 192 (1998).

[16] H. Vahlbruch, M. Mehmet, S. Chelkowski, B. Hage, A. Franzen, N. Lastzka, S. Goßler, K. Danzmann, and R. Schnabel, Phys. Rev. Lett. **100**, 033602 (2008).
[17] H. Vahlbruch, M. Mehmet, K. Danzmann, and R. Schnabel, Phys. Rev. Lett. **117**, 110801 (2016).
[18] K. Wakui, Y. Eto, H. Benichi, S. Izumi, T. Yanagida, K. Ema, T. Numata, D. Fukuda, M. Takeoka, and M. Sasaki, Sci. Rep. **4**, 4535 (2014).
[19] Z. Y. Ou, Phys. Rev. Lett. **77**, 2352 (1996).
[20] V. Giovannetti, S. Lloyd, and L. Maccone, Science **306**, 1330 (2004).
[21] L. Pezzé and A. Smerzi, Phys. Rev. Lett. **102**, 100401 (2009).
[22] V. Giovannetti and L. Maccone, Phys. Rev. Lett. **108**, 210404 (2012).
[23] L. Pezzé and A. Smerzi, Phys. Rev. Lett. **100**, 073601 (2008).
[24] M. D. Lang and C. M. Caves, Phys. Rev. Lett. **111**, 173601 (2013).
[25] M. D. Lang and C. M. Caves, Phys. Rev. A **90**, 025802 (2014).
[26] C. Sparaciari, S. Olivares, and M. G. A. Paris, J. Opt. Soc. Am. B **32**, 1354 (2015).
[27] C. Sparaciari, S. Olivares, and M. G. A. Paris, Phys. Rev. A **93**, 023810 (2016).
[28] L. Pezzé, A. Smerzi, G. Khoury, J. F. Hodelin, and D. Bouwmeester, Phys. Rev. Lett. **99**, 223602 (2007).
[29] B. T. Gard, C. You, D. K. Mishra, R. Singh, H. Lee, T. R. Corbitt, and J. P. Dowling, EPJ Quantum Technol. **4**, 4 (2017).
[30] J.-T. Shin, H.-N. Kim, G.-D. Park, T.-S. Kim, and D.-Y. Park, J. Opt. Soc. Korea **3**, 1 (1999).
[31] T. Nagata, R. Okamoto, J. L. O'Brien, K. Sasaki, and S. Takeuchi, Science **316**, 726 (2007).
[32] I. Afek, O. Ambar, and Y. Silberberg, Science **328**, 879 (2010).
[33] S. Ataman, Phys. Rev. A **97**, 063811 (2018).
[34] B. Yurke, S. L. McCall, and J. R. Klauder, Phys. Rev. A **33**, 4033 (1986).
[35] S. L. Braunstein and C. M. Caves, Phys. Rev. Lett. **72**, 3439 (1994).
[36] M. G. A. Paris, Int. J. Quantum Inf. **07**, 125 (2009).
[37] M. Jarzyna and R. Demkowicz-Dobrzański, Phys. Rev. A **85**, 011801 (2012).
[38] M. Takeoka, K. P. Seshadreesan, C. You, S. Izumi, and J. P. Dowling, Phys. Rev. A **96**, 052118 (2017).
[39] S. W. Brown, T. C. Larason, and Y. Ohno, Metrologia **47**, 02002 (2010).
[40] R. Schnabel, Phys. Rep. **684**, 1 (2017).
[41] D. Li, C.-H. Yuan, Z. Y. Ou, and W. Zhang, New J. Phys. **16**, 073020 (2014).
[42] U. Dorner, R. Demkowicz-Dobrzanski, B. J. Smith, J. S. Lundeen, W. Wasilewski, K. Banaszek, and I. A. Walmsley, Phys. Rev. Lett. **102**, 040403 (2009).
[43] T. Ono and H. F. Hofmann, Phys. Rev. A **81**, 033819 (2010).
[44] R. Demkowicz-Dobrzański, J. Kołodyński, and M. Guţă, Nat. Commun. **3**, 1063 (2012).